Affordable 3D Printed Microwave Antennas

Mohd Ifwat Mohd Ghazali, Eleazar Gutierrez, Joshua C. Myers, Amanpreet Kaur, Brian Wright, Premjeet Chahal
Department Electrical and Computer Engineering, Michgan State University
chahal@egr.msu.edu

Abstract

In this paper, a variety of 3D printed microwave antennas are presented including wide band, narrow band, multiband and reconfigurable designs. In particular, single layer patch, folded E-patch, a bilateral Vivaldi, Spartan logo and Lego-like assembled antennas are demonstrated. 3D printing provides significant flexibility in the design of antennas that combine the assembly of both dielectric and metal layers to achieve desired performance characteristics such as resonant frequency and radiation pattern. Also, small Lego-like blocks can be printed that allows in the design and assembly of novel antennas structures using a combination of dielectric and metal coated blocks.

I. Introduction

Three dimensional (3D) printing (additive process) technologies have gained significant interest over the past decade. It is attractive in research and development settings as prototypes can readily be produced with ease and at low cost [1]. This technology has been well studied for the design and fabrication of mechanical structures [2, 3]. The ability to print high resolution 3-dimensional geometries using a range of materials makes it ideal for the fabrication of complex microwave passive components, especially antenna elements. This is attractive as there is a significant demand for compact wireless systems which in turn require components that fit in small lattice space. Although traditional micromachining approaches can be used to fabricate such structures, however, these techniques require large capital investment and overall chemical and labor cost is high. Thus, 3D printing technology forms a cost effective and easy alternative to micromachining.

Recently, many microwave components including waveguides, horn antennas, and directional couplers have been demonstrated using 3D printing [4, 5]. Printing of microwave components is attractive as the dimensions of antennas, waveguides and other components is significantly large and existing technologies with printing resolution below 25μm can be used. With further development in materials and print head technologies, novel structures having interwoven metallic and dielectric regions (e.g., dielectric loaded antennas) can be readily manufactured using 3D printing. Also, cavities for chip integration within the antenna elements can be formed to design compact RF front-ends with improved performance.

This paper demonstrates several types of 3D printed microwave antennas which include a rectangular patch, logo based patch, folded E-patch and a wide band bilateral Vivaldi antenna. In the final section of this paper, a Lego-like reconfigurable antenna design is discussed based on the rearrangement of the physical structure. Unlike changing the resonance frequency by loading the antenna with electronic tuning elements (e.g., varactor diodes, MEMS) here small 3D Lego-like granules are used that can be rearranged to form complex 3D antennas of desirable geometrical shapes (interchangeable antenna) [6, 7]. As an example, a simple monopole antenna can be transformed into a folded antenna just by rearranging the granules. Thus, a new design is quickly obtained while avoiding the difficult remanufacturing process. This approach allows antennas to be designed and tested prior to mass production.

II. Design and Fabrication

The simulation and optimization of the antenna elements was carried out using a commercial FEM solver HFSS. After evaluating the simulation results and obtaining the desirable performance characteristic, the design file is converted and exported to Stratasys Object Connex350 3D printer using SolidWorks for fabrication. The printer uses multi-jetting technology and has the capability of 16 μm print resolution. It also has the ability to use variety of polymer-based material that allows flexibility in designing antennas on different substrates. Upon curing "Vero White" resin is a rigid opaque photopolymer that is used here to print the antennas. This material is chosen based on its durability and strength and relatively low loss dielectric characteristics compared to other available materials. In the simulations, the following dielectric properties ε_r = 2.4-2.6 and a tan δ = 0.02 are used. These material parameters were determined through measurements. The dielectric constant value was found to be strongly dependent on the porosity of the material. The base material used in the fabrication for all the antennas is a light weight plastic. The fabricated 3D structure were metal coated to form conductive regions where needed. They were coated with titanium (Ti, 250nm) and copper (Cu, 1 μm) layers using Denton Vacuum Desktop Pro sputtering system. In place of vacuum deposition, electroless plating can also be used to deposit copper on the plastic parts.

III. Design and Simulation of Patch Antennas

First narrow band and multi-band patch antennas were designed and fabricated, and these results are presented in this section.

a. Rectangular Patch Antenna

Microstrip patch antennas are one of the most widely used antennas because of their simplicity of design, lightweight and low profile [8]. Figure 1 shows the HFSS structure used for simulating the 3D patch antenna. The structure consists of a "Vero White" dielectric substrate sandwiched between a metalized ground plane at the bottom and a metalized radiating patch at the top. The HFSS simulation shows that the patch antenna operates at 5.45 GHz. To fabricate the patch, the structure is 3D printed and followed by Cu metallization on one side. A coax cable with SMA connector was attached from the back side and the center conductor was affixed to the

top metal layer using silver epoxy. The picture of an assembled 3D printed patch antenna is shown in Figure 2. The reflection coefficient of the metalized patch antenna is measured using Agilent N5227A network analyzer. The operational frequency is measured to be 5.48 GHz with a minimum value of approximately -20dB. A comparison of reflection coefficients between the fabricated patch antenna and the simulated patch antenna is shown in Figure 3. The result shows very good agreement between these results. The slight difference in operational frequencies is likely due to the air gap that may be present between the ground plane and the dielectric layer. In addition, Figure 4 shows the simulated gain of this patch antenna at 5.45 GHz. Gain of 6.94 dB is achieved at this resonance frequency.

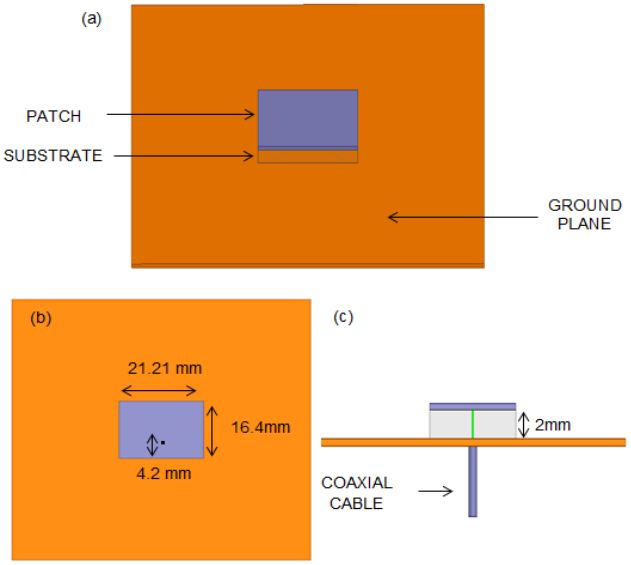

Figure 1. 3D patch antenna design (a) 3D view (b) Top view and (c) Side view.

Figure 2. Fabricated and metalized 3D printed Patch Antenna.

b. Logo Patch Antenna (Spartan block 'S')

Three dimensional printing has the ability to fabricate complex shapes in one piece and this aspect can be used for designing of logo (or brand name) antennas [9, 10]. Michigan State University is known for its Spartan logo which looks like a letter 'S' as shown in Figure 5. The size of the structure is optimized for desired resonance frequency. The position of the feed pin is optimized using HFSS to achieve narrow band operation. The material and thickness of the substrate is the same as the previous patch antenna. Figure 6 (a) shows the printed 'S' structure before metallization, and Figure 6 (b) shows after metallization and assembly on a copper plate and coax cable connection. Here also only the top surface was metalized with sputtered Cu. Figure 7 shows the measured and simulated reflection coefficients, S_{11}, of the antenna. Since the printed 'S' structure is directly placed on the copper plate there is a small air gap present at the interface. The effect of air gap on the S_{11} was also simulated and results also shown in Figure 7. From the results it is evident that the resonance frequency increases with increase in air gap. In other words, the effective dielectric constant of the dielectric layer decreases. Figure 8 shows the simulated radiation pattern of the Spartan letter "S" antenna which gives a maximum gain of 2.9 dB at 2.68 GHz.

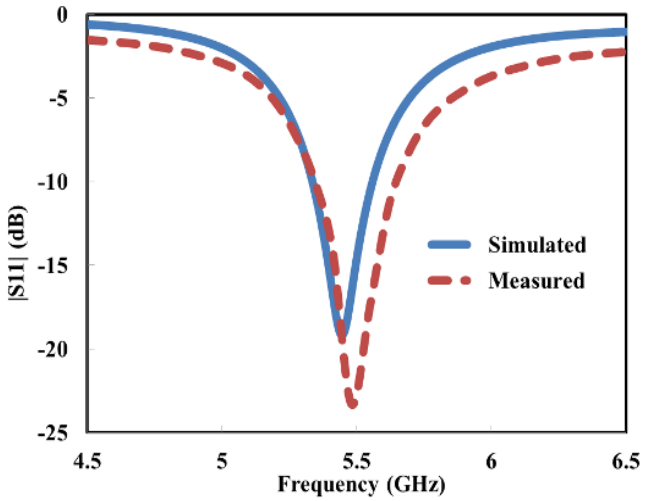

Figure 3. Simulated and measured of 3D printed patch antenna for reflection coefficient, S_{11}.

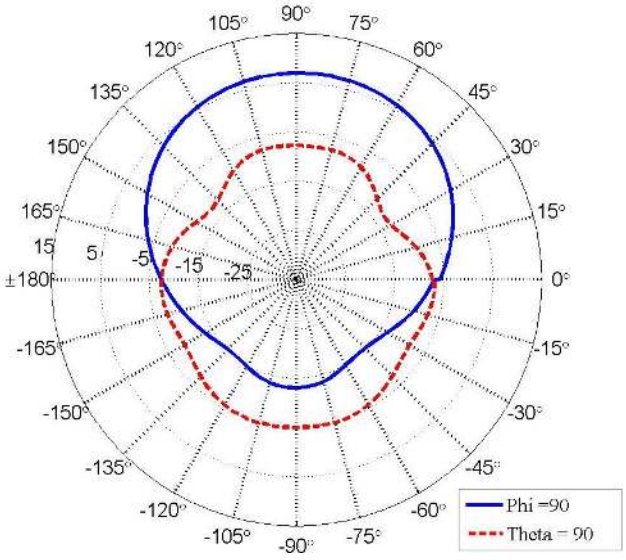

Figure 4. The simulated E- and H-plane radiation pattern of the 3D printed rectangular patch antenna at 5.45 GHz.

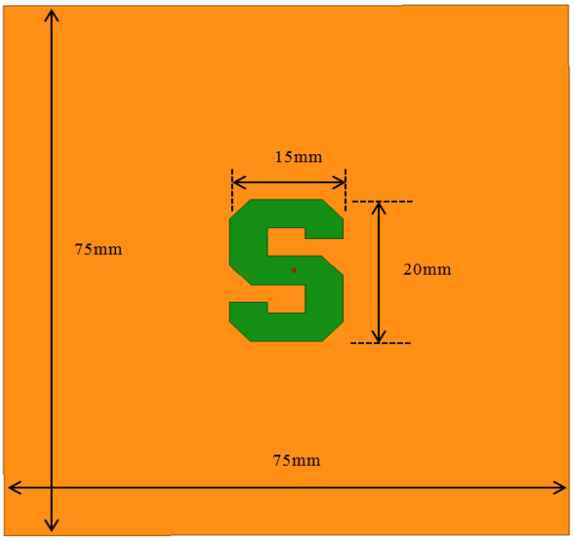

Figure 5. 3D Spartan 'S' logo patch antenna design.

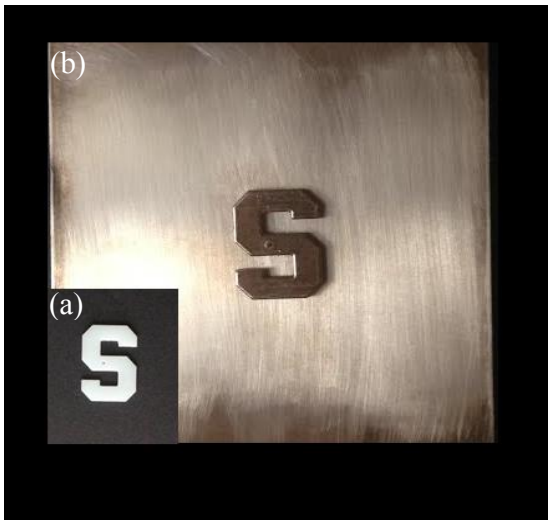

Figure 6. 3D printed Spartan 'S' logo (a) unmetalized (b) metalized with copper platting as the ground.

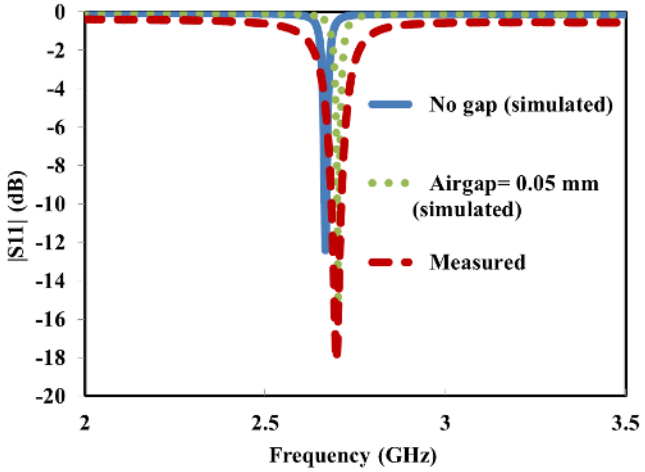

Figure 7. Simulated and measured reflection coefficient, S_{11} of 3D printed Spartan 'S' logo with simulation for air gap.

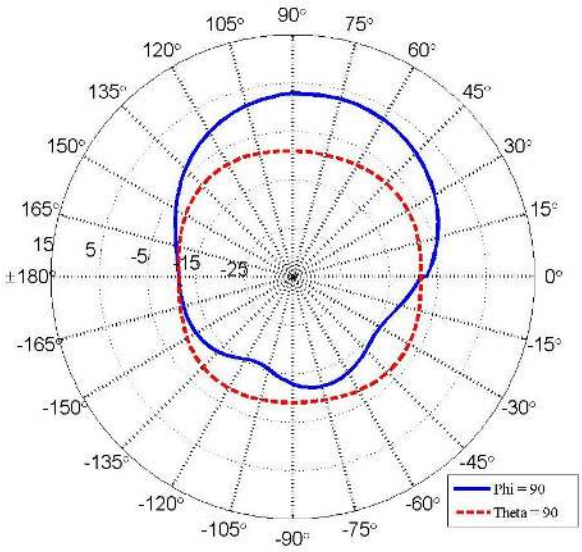

Figure 8. The simulated radiation pattern on the E- and H-plane of the Spartan 'S' logo patch antenna at 2.68GHz.

c. Logo Patch Antenna (Spartan helmet)

Due to limited space in electronic devices, having a single functional narrowband antenna will limit its capability. To overcome this limitation, a multiband antenna is desirable [11]. Many designs have been studied in order to improve the performance of multiband antennas such as multilayer patch antennas, [12], as an example. Such antenna structures can readily be fabricated using 3D printing. In a multiband design antenna multiple current paths are necessary. This can be achieved by using notch structures that can readily be 3D printed. Another one of Michigan State University logos, 'The Spartan Helmet' can be used to design a multiband antenna element. Figure 9 shows a fabricated Spartan Helmet logo antenna after metallization and assembly.

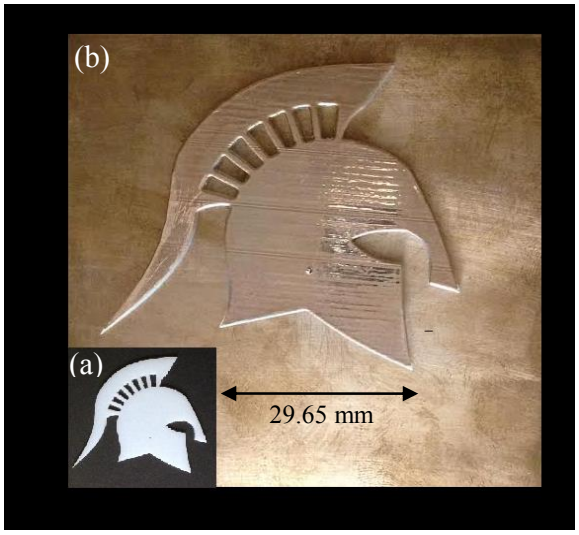

Figure 9. 3D printed Spartan Helmet logo (a) before metallization and (b) after metallization and assembly.

Figure 10 shows the simulated and measured multiband operational frequencies (S_{11}) of this structure. The results

match closely with each other. Slight discrepancy is largely due to the presence of small air gap between the dielectric and the ground metal. The shape of the crest and the face plate sections of the Spartan helmet were determined to have a strong effect on these resonant frequencies and these sections were optimized to achieve multiband operation. The simulated radiation pattern of this antenna at the second resonance frequency is shown in Figure 11. A gain of approximately 3.35 dB at 2.23 GHz is achieved for this design.

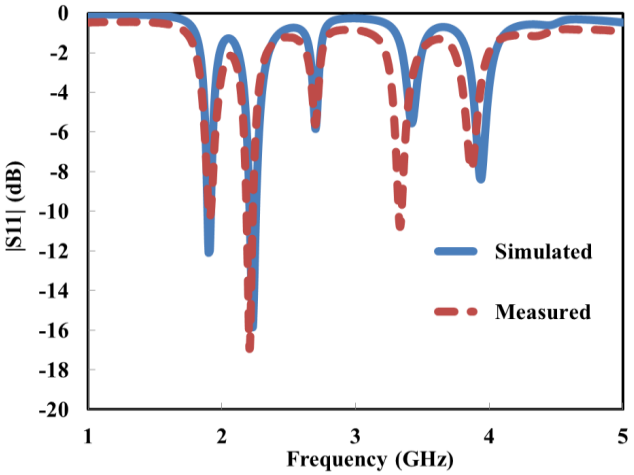

Figure 10. Simulated and measured reflection coefficient, S_{11} of 3D printed 'Spartan Helmet' logo.

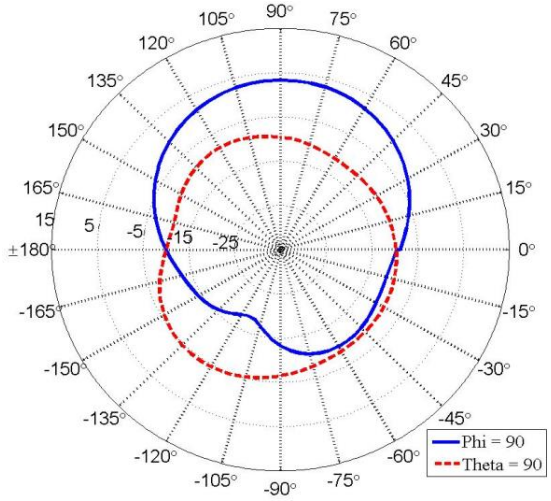

Figure 11. The simulated E- and H-plane radiation pattern of the Spartan Helmet antenna at 2.23 GHz.

IV. Design and Simulation of Wide Band Antennas

Two types of wide band antennas are demonstrated: a) Folded E-patch and b) Vivaldi antenna.

a. Folded E-Patch Antenna

Here a folded E-patch antenna with two cylindrical support structure on the edge was designed based on Ref. [13]. In the designs presented above the 3D printed "Vero White" polymer was used as the dielectric material for the antennas. Here, in this design, the dielectric material is used as a support material and is coated with a thin metal layer and air acts as the dielectric layer. The folded E-patch antenna is designed for wideband applications. The length of the three arms of the folded patch antenna allows in the tailoring of resonance frequency and bandwidth. Figure 12 and Table 1 shows the dimensions used in simulation and fabrication.

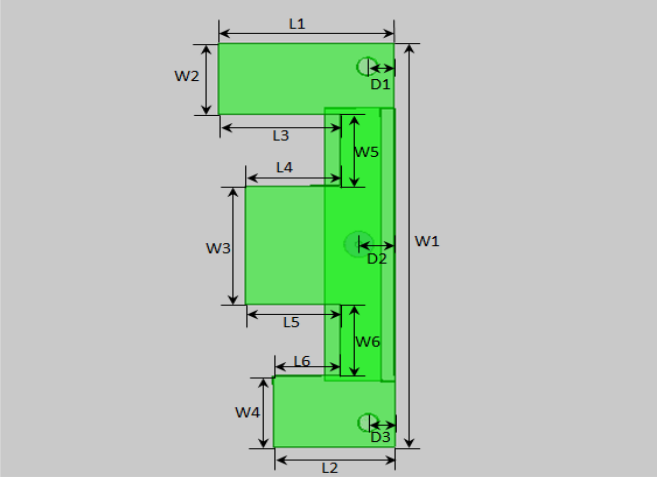

Figure 12. The geometry of the Folded E-Patch (top view).

Table 1. Dimensions of the folded E-patch antenna.

Parameters	Values
L1	13mm
L2,L3	9mm
L4,l5	7mm
L6	5mm
W1	34mm
W2	6mm
W3	10mm
W4,W5,W6	6mm
D1,D3	2mm
D2	2.7mm

The fabricated structure after metallization (Ti/Cu layers) and assembly is shown in Figure 13. Here, unlike the previous designs above, the ground plane was also 3D printed and coated with thin metal film. Figure 14 shows the measured and simulated S_{11} of the antenna. There is a significant difference between these results. The antenna operates over a wide frequency band. However, the resonance frequency of the fabricated antenna is shifted to higher frequencies because of fabrication tolerances. The polymer material has low glass transition temperature and thus the structure deformed during metallization in the sputtering machine. In the design, the E-patch region is parallel to the ground plane, whereas there is a slight angle in the fabricated structure, i.e., the structure droops down slightly. Use of low temperature metal deposition or the use of a high temperature polymer material can help overcome this challenge.

Figure 15 shows the measured and simulated results of an E-patch antenna in which the cylindrical posts are made of dielectric, i.e., not coated with metal film. This affects the flow of current on the antenna element and thus changes the operating frequency. This result shows that a combination of metal and non-metalized 3D printed structures can be used in the design of novel antenna elements.

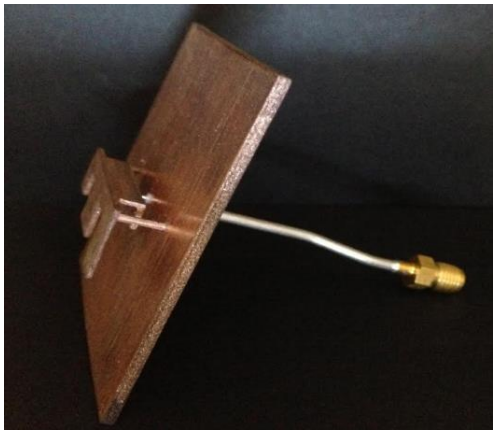

Figure 13. 3D printed folded E-patch antenna after metallization and assembly. The structure is supported by two cylindrical posts on the ends.

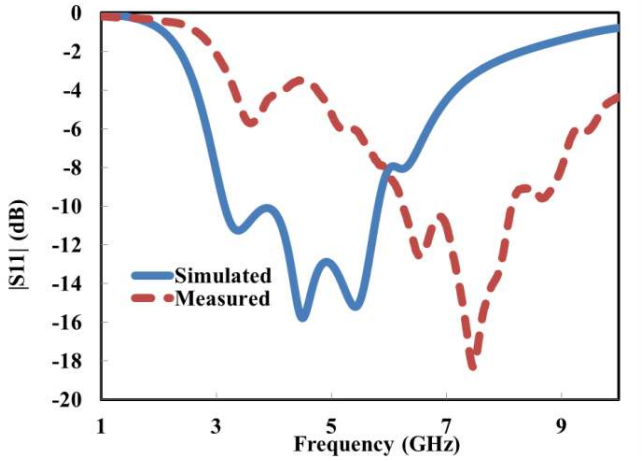

Figure 14. Simulated and measured reflection coefficient of a full metalized copper folded E-patch antenna.

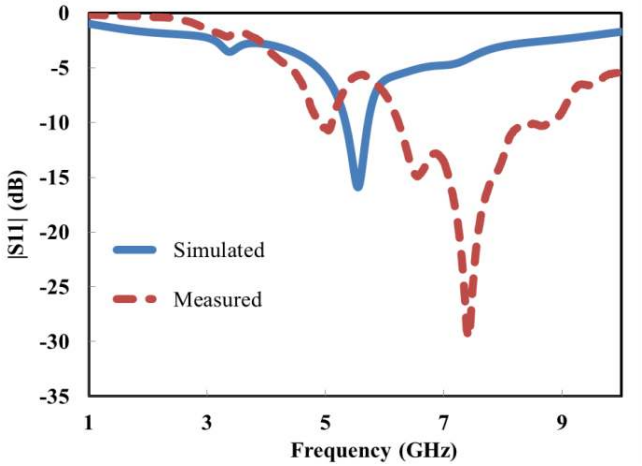

Figure 15. Simulated and measured reflection coefficient of a partially metalized copper folded E-patch antenna.

b. Bilateral Vivaldi Antenna

Vivaldi antennas are well known for ultra-wideband frequency operation. It acts like an end-fire traveling wave antenna. Other than the wideband characteristics, it also has a relatively high gain and consistent radiation pattern over a wide frequency range. The most common Vivaldi antenna is a planar structure which requires multi-layer structure to fabricate. With the help of 3D printing technology a Vivaldi antenna fabrication can be simplified and more importantly high gain antennas can be designed.

Here a bilateral Vivaldi antenna is designed based on modification of a normal Vivaldi antenna [14]. The design dimensions are shown in Figure 16. The antenna has a cavity region with a cover to reduce radiation from the back side. The front side is slowly tapered to achieve wide band operation. A coaxial is fed from the side and the inner and outer conductors of the coax are connected on the opposite ends of the slot. Figure 17 shows the 3D printed structures before and after metallization. The bilateral Vivaldi antenna is printed in two separate pieces so that the coaxial cable can be easily inserted and also the metallization can be easily carried out in the cavity region. Cavities in the structure can be formed to allow direct packaging of chips within the antenna element. The pin and holes in the structures are used as a guide for alignment of the two separate sections.

The simulated and measured reflection coefficient of the antenna is shown in Figure 18. These results match closely with the exception of additional resonances in the measured result. This can largely be attributed to the coaxial mount. The impedance matching was determined to be sensitive to the coax center pin location in the slot. In the simulation, the location of the coax center pin is optimized to give the best reflection coefficient possible. However, during fabrication it is difficult to attain a perfect match as the coax is mounted manually.

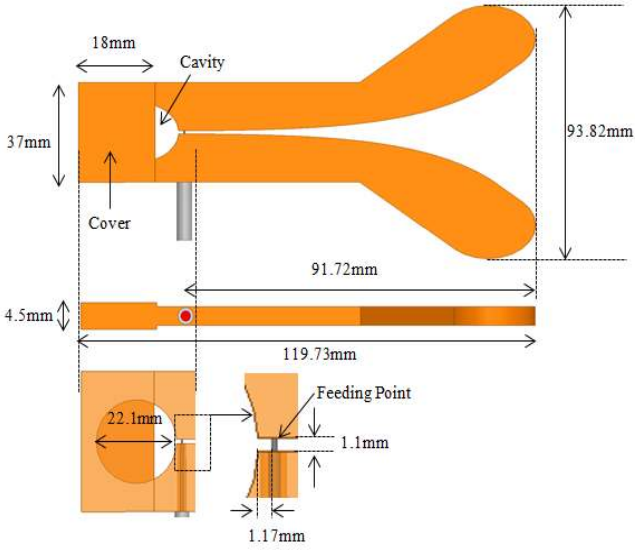

Figure 16. Design parameters of the proposed bilateral antenna. The circular cavity is partially covered on both sides to reduce back radiation.

Figure 19 shows the measured and simulated gain of the Vivaldi antenna. The antenna has a high gain over a wide frequency range. A cover on the cavity region was introduced to enhance the gain of the antenna by reducing back side radiation lobe. This cover can readily be fabricated using 3D printing as opposed to conventional fabrication techniques.

The measured gain of the antenna is less than the simulated antenna, around 2 to 4 dB lower. This can be attributed to geometrical and material factors. The location of the feed point in the slot and the exact dimension of the slot have a significant effect on gain of the antenna. Furthermore, the coax center pin was attached to the structure using silver paste which is known to have high loss at higher frequencies and thus it introduces series parasitic resistance. Also, the plastic printed structure has high surface roughness. Surface roughness of approximately 15μm was measured on these printed parts. Even with significant loss, the overall measured gain of the antenna is very high as expected for Vivaldi antennas.

Figure 17. Fabricated 3D printed Bilateral Vivaldi Antenna before and after metallization, prior to assembly.

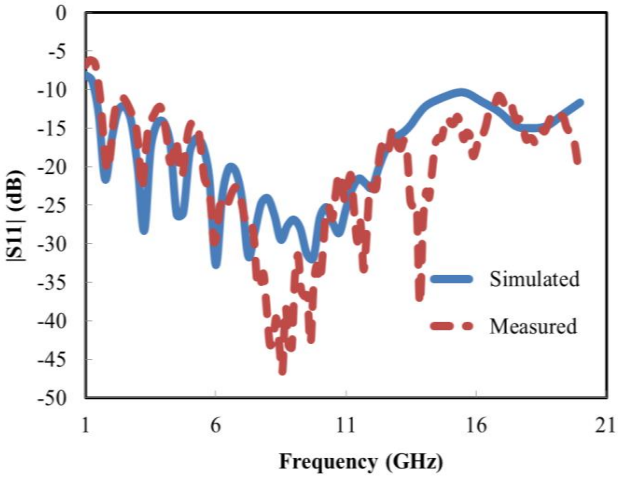

Figure 18. Simulated and measured reflection coefficient of 3D printed Bilateral Vivaldi Antenna.

Figure 20 shows the radiation pattern at 10 GHz determined through simulations. It shows that the radiation pattern is symmetrical and has low side lobes. Also, the back radiation is low which helps enhance gain. These results show that high gain, wide band Vivaldi antennas can be fabricated through 3D printing. Further enhancement in these results can be expected by improving the printing tolerance and reducing surface roughness.

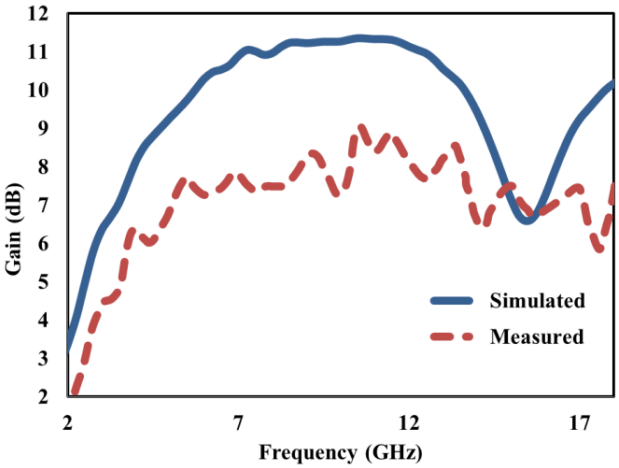

Figure 19. Simulated and measured maximum gain versus frequency for 3D printed Bilateral Vivaldi Antenna.

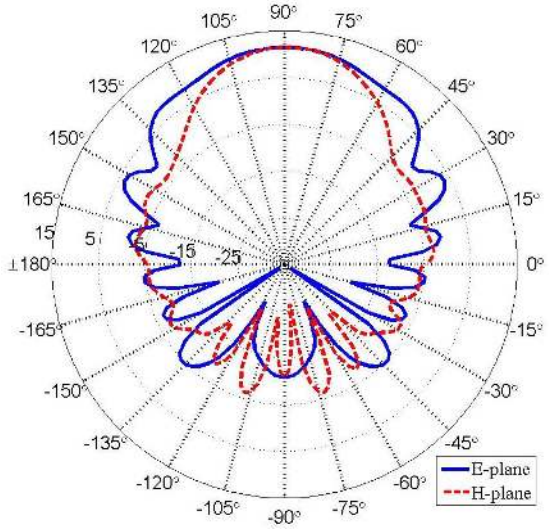

Figure 20. The simulated E- and H-plane radiation pattern of the Vivaldi Antenna at 10GHz.

V. Design and Simulation of Reconfigurable Antenna

A reconfigurable antenna design is demonstrated by antenna build using Lego-like blocks.

3D printed Granules for Lego-like antennas

From the above discussion, it is clear that dielectric can be used as a part in antenna design. In this section, a new type of Lego-like antenna structure is presented that can be physically reconfigured to operate at any desired frequency. Here the dielectric or metalized granular brick like structures can be assembled together to form any shape. The starting structure is a 3D printed folded dipole and it is loaded with these granular structures to change the operating frequency of the antenna.

Figure 21(a-d) shows four simple designs in which the metallized and non-metallized parts are assembled together on top of a folded dipole antenna. Figure 21(e) shows the photomicrograph of fabricated granular blocks of which one is metalized with Cu on all sides. Figure 22 shows the simulated reflection coefficient of the folded antenna, first, second and third design of 3D folded antenna. By rearranging the dielectric and metallic blocks the resonance frequency can be

changed. The reference structure of the 3D folded antenna shows the operational frequency of 2.81 GHz. By adding the 3D block structures, the frequency is shifted and the new operating frequencies are 1.84 GHz, 1.71 GHz and 1.61 GHz for the three structures shown in Figure b – d, respectively. One of the main challenges with this design is that there is significantly high contact resistance between the metalized blocks due to poor connection. This can be reduced with improvement in surface roughness and better metal adhesion to "Vero White" polymer material.

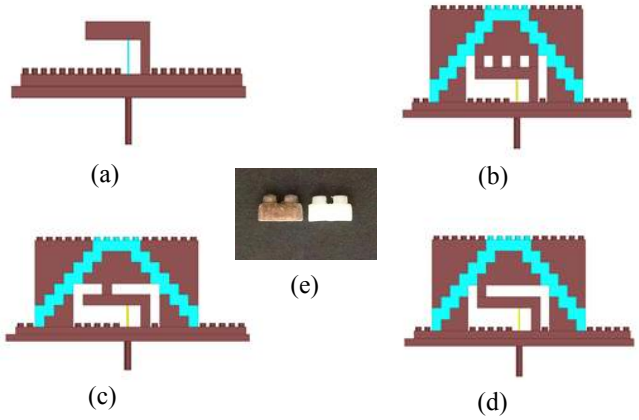

Figure 21. Lego-like conductive and dielectric blocks can be arranged on top of a folded dipole to achieve desired operating frequency. (a) Reference structure for 3D folded antenna, (b) 1st design, (c) 2nd Design, (d) 3rd Design. (e) Shows printed Lego-like granular blocks where one is metallized on all sides.

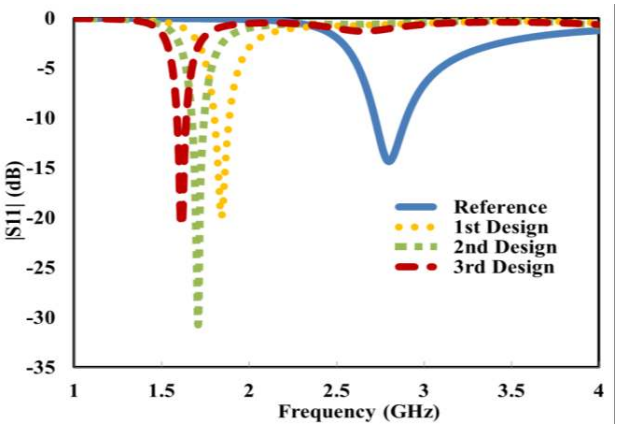

Figure 22. Simulated reflection coefficient of 3D folded antennas.

Conclusions

This paper provides many examples of 3D printed antenna elements that can readily be fabricated using existing technologies. Antennas with narrow band, multiband and wide band operations are demonstrated. The simulation, fabrication, and experimental results are presented in a way to show the practical application with the different antenna shapes that suit different applications. It is also shown that 3D printing allows in the fabrication of complex granular parts that can be assembled together to form Lego-like antennas. With further development in 3D printing, the RF front-end chips can be embedded within the antenna element making future wireless systems compact and low-cost.

Acknowledgments

Special thanks to EM group members from Michigan State University for helpful discussions.

References

1. P.M. Dickens, "Research developments in rapid prototyping," in *Proceedings of the Institution of Mechanical Engineers, Part B: Journal of Engineering Manufacture 209*, August, 1995, pp. 261-266
2. I. Gibson, T. Kvan, L. Wai Ming, "Rapid prototyping for architectural models," *Rapid Prototyping Journal*, vol. 8, no. 2, pp. 91-95, 2002.
3. H. Kodama, "Automatic method for fabricating a three-dimensional plastic model with photo-hardening polymer," *Review of Scientific Instruments*, vol. 52, no. 11, pp. 1770-1773, 1981.
4. O.S. Kim, "Rapid Prototyping of Electrically Small Spherical Wire Antennas," *Antennas and Propagation, IEEE Transactions*, vol. 62, no. 7, pp. 3839-3842, 2014.
5. U. Schwarz, M. Helbig, J. Sachs, F. Seifert, R. Stephan, F. Thiel, and M.A. Hein "Physically small and adjustable double-ridged horn antenna for biomedical UWB radar applications," in *IEEE ICUWB 2008*, Hannover, Sept. 10-12, 2008, pp 5-8.
6. M.N.M. Kehn, Ó. Quevedo-Teruel, and E. Rajo-Iglesias. "Reconfigurable loaded planar inverted-F antenna using varactor diodes,"*Antennas and Wireless Propagation Letters, IEEE*, vol. 10, pp. 466-468, 2011.
7. S. Zhu, T.S. Ghazaany, R.A. Abd-Alhameed, S.M.R. Jones, J. Noras, T. Suggett, and S. Marker. "Miniaturized tunable conical helix antenna," in *Radio and Wireless Symposium (RWS),* Jan 19-23, 2014, pp. 100-102.
8. C.A. Balanis, *Antenna theory: analysis and design*, John Wiley & Sons, 2002.
9. Y.L. Chow, and C. W. Fung, "The city university logo patch antenna," in *Proc. Asia Pacific Microwave Conference*, Vol. 1, Dec. 2-5, 1997, pp. 229-232.
10. C.Y.D. Sim and C.J. Chi. "A circularly polarized olympic-like logo antenna for 900 MHZ UHF RFID reader," *Microwave and Optical Technology Letters,* vol. 55, no. 6, pp. 1358-1360, June 2013.
11. K. L. Wong. *Compact and broadband microstrip antennas*. Vol. 168. John Wiley & Sons, 2004.
12. K. Lim, S. Pinel, M. Davis, A. Sutono, C.H. Lee, D. Heo, A. Obatoynbo, J. Laskar. J.M. Tantzeris, R. Tummala, "RF-system-on-package (SOP) for wireless communications," *IEEE Microwave Magazine*, Vol. 3, no. 1, pp. 88-99, March 2002.
13. H. Malekpoor, and J. Shahrokh, "Ultra-wideband shorted patch antennas fed by folded-patch with multi resonances," *Progress In Electromagnetics Research B* 44, pp 309-326, 2012.
14. F. Lin, Y. Qi, and Y.C. Jiao, "A 0.7–20-GHz strip-fed bilateral tapered slot antenna with low cross polarization," *IEEE Antennas and Wireless Propagation Letters,* vol. 12, pp. 737-740, 2013.